Numerical simulation of dynamic brittle fracture of pipeline steel subjected to DWTT using XFEM-based cohesive segment technique

Reza H. Talemi

ArcelorMittal Global R&D Gent-OCAS NV, Pres. J.F. Kennedylaan 3, 9060 Zelzate, Belgium
Reza.HojjatiTalemi@ArcelorMittal.com

ABSTRACT. In the past several numerical studies have addressed the ductile mode of fracture propagation. However, the brittle mode of pipeline failure has not received as much attention yet. The main objective of this study is to predict brittle fracture behaviour of API X70 pipeline steel by means of a numerical approach. To this end, the eXtended Finite Element Method (XFEM)-based cohesive segment technique is used to model Drop Weight Tear Test (DWTT) of X70 pipeline steel at -100°C. In this model the dynamic stress intensity factor and crack velocity are calculated at the crack tip at each step of crack propagation.

KEY WORDS: Dynamic brittle fracture; Pipeline steel; DWTT; XFEM; Cohesive segment.

INTRODUCTION

Concerns have been raised that leaks in a CO_2 pipeline could escalate to brittle fracture crack propagation, due to the large temperature drop associated with the expansion of dense phase CO_2 to ambient conditions [1]. In order to avoid a long running brittle fracture minimum requirements for the shear area in a DWTT are specified. There are many studies aimed to develop Finite Element (FE) models to describe the impact phenomena [2-4]. Wu et al. [2] used the Gurson-Tvergaard-Needleman (GTN) model to simulate the fracture behaviour during DWTT. They analysed the equivalent stress, nucleation of voids and void size distribution using their FE Model. They reported that the fracture propagates in a triangular shape at the crack tip, and inverse fracture occurs when the fracture propagated about 3/4 of sample width. They found that in some of their simulations the transition during DWTT is from the brittle to the ductile and then again to the brittle zone. Scheider et al. [3] have simulated ductile dynamic fracture propagation using a numerical approach with application of damage mechanics models and a cohesive zone method. Basically they used the GTN model to simulate the DWTT with pressed notch and pre-fatigued crack. They have derived numerical fracture resistance curves employed for the assessment of ductile fracture resistance. Nonn et al. [4] modelled the ductile fracture behaviour of API X65Q pipeline steels subjected to DWTT using the GTN model. They have applied their model to describe and evaluate dynamic crack propagation in DWTT and pipe.

The majority of available studies in the literature, including the above reviewed ones, concentrated on numerical modelling of ductile behaviour of materials. There are limited studies that focus on brittle fracture of the DWTT or Charpy V-Notch (CVN) impact tests at low temperatures. For instance Sainte Catherine et al. [5] have developed the Beremin (1983) cleavage model to simulate CVN and Sub-Size CVN impact tests at low temperature (-90°C). From their study they found that the results showed a good transferability potential. More recently, Hojjati-Talemi et al. [6] have implemented a novel

approach of the XFEM-based cohesive segment technique to simulate dynamic brittle fracture of pipeline steel subjected to CVN loading conditions.

In the present work, a 2D finite element model was developed to represent the actual practice of DWTT. To this end the XFEM-based cohesive segment technique was used to model dynamic brittle fracture behaviour of API X70 pipeline steel. After validation of the developed model against experimental observations, significant results from the simulation are presented and discussed.

EXPERIMENTAL

Material

The material used in this research was API X70 grade CO_2 pipeline steel. The mechanical properties of the pipe were measured using round tensile bars with a diameter of 8 mm. To machine the tensile samples, a test plate was taken from the original pipe. All tests were carried out at different temperatures ranging from room temperature to -100°C under a low displacement rate of 0.036 mm/s. These data were subsequently used to determine the nominal and true stress–strain properties of the X70 steel grade. The average mechanical properties of X70 steel grade measured at room temperature (RT) are set out in Tab. 1.

Temperature [°C]	Yield strength [σ_y, MPa]	Young's Modulus [E, GPa]
20	520	210
-100	760	210

Table 1: Mechanical properties of steel X70 at room and sub-zero temperatures.

DWTT

DWTT is a material characterisation test aimed at avoiding brittle fracture and ensuring crack arrest in pipelines (seamless or welded). In a DWTT, the test specimen is a rectangular bar with a length of 305 mm, a width of 76 mm and of the full material thickness (up to at least 19 mm). The specimen has a shallow pressed notch and is subjected to three-point bending impact load, as shown in Fig. 1. The standards specify a 5 mm deep notch made by a sharp indenter with a 45° included angle resulting in a tip radius that is normally between 0.0127 to 0.0254 mm.
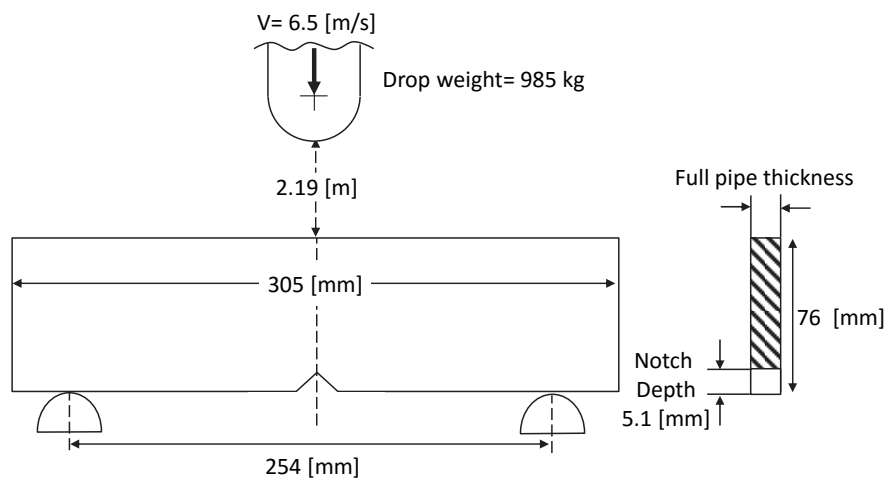

Figure 1: Dimensions of DWTT specimen along with the impact loading conditions. In this study thickness of 19 mm was used for DWTT specimen.

A series of specimens are broken under impact loading at various temperatures and the proportions of ductile fracture (shear) and brittle fracture (cleavage) on the fracture surfaces are measured. From correlations with full-scale pipe burst tests, the transition temperature corresponding to about 85 percent shear is normally defined in application standards as the fracture propagation transition temperature.

XFEM-BASED COHESIVE SEGMENT

XFEM principles

XFEM approach was first introduced by Belytschko and Black [7]. It is an extension of the conventional finite element method based on the concept of partition of unity, which allows local enrichment functions to be easily incorporated into a finite element approximation. Crack modelling based on XFEM allows for simulation of both stationary and moving cracks. Simulation of propagating cracks with XFEM does not require initial crack and crack path definitions to conform to the structural mesh. The crack path is solution dependent i.e., it is obtained as part of the solution. Cracks are allowed to propagate through elements allowing for modelling of fracture of the bulk material. For the purpose of fracture analysis, the enrichment functions typically consist of the near-tip asymptotic functions that capture the singularity around the crack tip and a discontinuous function that represents the jump in displacement across the crack surfaces. The approximation for a displacement vector function u with the partition of unity enrichment is

$$u = \sum_{I=1}^{N} N_I(x) \left[u_I + H(x)a_I + \sum_{\alpha=1}^{4} F_\alpha(x) b_I^\alpha \right]$$

(1)

where $N_I(x)$ are the usual nodal shape functions; the first term on the right-hand side of the above equation, u_I, is the usual nodal displacement vector associated with the continuous part of the finite element solution; the second term is the product of the nodal enriched degree of freedom vector, a_I, and the associated discontinuous jump function $H(x)$ across the crack surfaces; and the third term is the product of the nodal enriched degree of freedom vector, b_I^a, and the associated elastic asymptotic crack-tip functions, $F_a(x)$. The first term on the right-hand side is applicable to all the nodes in the model; the second term is valid for nodes whose shape function support is cut by the crack interior; and the third term is used only for nodes whose shape function support is cut by the crack tip. The discontinuous jump function across the crack surfaces, H(x), can be written as

$$H(x) = \begin{cases} 1 & if (x - x^*).n \geq 0, \\ -1 & otherwise, \end{cases}$$

(2)

where x is a sample (Gauss) point, x^* is the point on the crack closest to x, and n is the unit outward normal to the crack at x^*. The asymptotic crack tip functions in an isotropic elastic material, $F_a(x)$, are given by

$$F_\alpha(x) = \left[\sqrt{r} \sin\frac{\theta}{2}, \sqrt{r} \cos\frac{\theta}{2}, \sqrt{r} \sin\theta \sin\frac{\theta}{2}, \sqrt{r} \sin\theta \cos\frac{\theta}{2} \right]$$

(3)

where (r, θ) is a polar coordinate system with its origin at the crack tip and $\theta = 0$ is tangent to the crack at the tip. These functions span the asymptotic crack-tip function of elasto-statics, and $\sqrt{r} \sin(\theta/2)$ takes into account the discontinuity across the crack face. Accurately modelling the crack-tip singularity requires constantly keeping track of where the crack propagates and is cumbersome because the degree of crack singularity depends on the location of the crack in a non-isotropic material. Therefore, the asymptotic singularity functions can only be used when modelling stationary cracks.

Cohesive segment principles

One of the approaches within the framework of XFEM is based on traction-separation cohesive behaviour. This approach is used to simulate crack initiation and propagation. This is a very general interaction modelling capability, which can be used for modelling brittle or ductile fracture. The XFEM-based cohesive segments method can be used to simulate crack initiation and propagation along an arbitrary, solution-dependent path in the bulk material, since the crack propagation is not tied to the element boundaries in a mesh. In this case the near-tip asymptotic singularity is not needed, and only the displacement jump across a cracked element is considered. Therefore, the crack has to propagate across an entire element at a time to avoid the need to model the stress singularity. More information can be found in the author's previous work [6].

The formulae and laws that govern the behaviour of XFEM-based cohesive segments for a crack propagation analysis are very similar to those used for cohesive elements with traction-separation constitutive behaviour. The similarities extend to

the linear elastic traction-separation model, damage initiation criteria, and damage evolution laws. Damage modelling allows simulating the degradation and eventual failure of an enriched element. The failure mechanism consists of two portions: a damage initiation criterion and a damage evolution law. The initial response is assumed to be linear. However, once a damage initiation criterion is met, damage can occur according to a user-defined damage evolution law. Damage of the traction-separation response for cohesive behaviour in an enriched element is defined within the same general framework used for conventional materials. However, it is not needed to specify the undamaged traction-separation behaviour in an enriched element.

Damage initiation refers to the beginning of degradation of the cohesive response at an enriched element. The process of degradation begins when the stresses or the strains satisfy specified damage initiation criteria. In this study the maximum principal stress criterion was used in order to model crack initiation. The maximum principal stress criterion can be represented as

$$f = \left\{ \frac{\langle \sigma_{\max} \rangle}{T_{\max}} \right\} \tag{4}$$

Here, T_{max} represents the maximum allowable principal stress. The symbol $\langle \sigma_{\max} \rangle$ represents the Macaulay bracket with the usual interpretation (i.e., $\langle \sigma_{\max} \rangle = 0$ if $\sigma_{max} < 0$ and $\langle \sigma_{\max} \rangle = \sigma_{max}$ if $\sigma_{max} \geq 0$). The Macaulay brackets are used to signify that a purely compressive stress state does not initiate damage. Damage is assumed to initiate when the maximum principal stress ratio (as defined in the expression above) reaches a value of one. Afterwards an additional crack is introduced or the crack length of an existing crack is extended after equilibrium increment when the fracture criterion, f, reaches the value 1.0 within a given tolerance f_{tol}:

$$1.0 \leq f \leq 1.0 + f_{tol}$$

If $f \geq 1 + f_{tol}$ the time increment is cut back such that the crack initiation criterion is satisfied. In this study the value of f_{tol} was specified as 0.05.

The damage evolution law describes the rate at which the cohesive stiffness is degraded once the corresponding initiation criterion is reached. A scalar damage variable, D, represents the averaged overall damage at the intersection between the crack surfaces and the edges of cracked elements. It initially has a value of 0. If damage evolution is modelled, D monotonically evolves from 0 to 1 upon further loading after the initiation of damage. The normal and shear stress components are affected by the damage according to

$$t_n = \begin{cases} (1-D) T_n & \text{if } T_n \geq 0 \\ T_n & \text{otherwise} \end{cases} \tag{5}$$

$$t_s = (1-D) T_s \tag{6}$$

$$t_t = (1-D) T_t \tag{7}$$

where T_n, T_s and T_t are the normal and shear stress components predicted by the elastic traction separation behaviour for the current separations without damage. To describe the evolution of damage under a combination of normal and shear separations across the interface, an effective separation is defined as

$$\delta_{\max} = \sqrt{\langle \delta_n \rangle^2 + \delta_s^2 + \delta_t^2} \tag{8}$$

Concerning the damage variable D, an exponential model has been adopted to describe its evolution. In particular, according to such model, the following relation holds

$$D = \int_{0}^{\delta_{\max}} \frac{T_{\max}}{\Gamma} d\delta \qquad (9)$$

in which, T_{max} indicates the cohesive stress and δ the effective displacement. In addition, Γ represents the cohesive energy, while δ_{max} is the effective displacement at complete failure. In terms of crack propagation direction, whenever the crack initiation criterion (maximum principal stress criterion) was specified, the newly introduced crack was defined to be always perpendicular to the maximum principal stress direction when the fracture criterion is satisfied.

FINITE ELEMENT MODELLING

Model description

I n this study the DWTT configuration was modelled using ABAQUS software. The model consists of four parts, namely a hammer, two anvils and the DWTT specimen which can be meshed independently. Fig. 2 illustrates the finite element mesh of the specimen and an assembled view of the model.
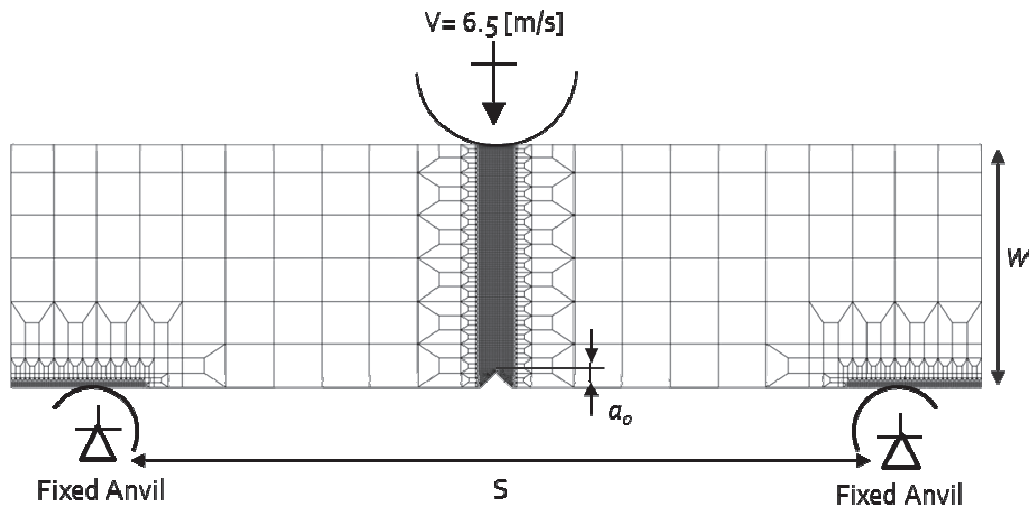

Figure 2: FE mesh along with boundary and loading conditions of DWTT.

A two-dimensional, 4-node (bilinear), plane strain quadrilateral, reduced integration element (CPE4R) was used in order to model the test configuration. A fixed rigid contour line represents the anvils and the hammer. The specimen is put on two rigid anvils and the hammer impacts the specimen under three point bending loading conditions. A mesh size of 0.5mm × 0.5mm was considered at the potential crack propagation regions and increased gradually far from the area of interest. Moreover, to capture correctly the multiaxial stress gradient at the notch tip the mesh size was decreased down to 0.05mm in this region.

Contact was defined between the hammer and the specimen, as well as between the specimen and the anvils using a Coulomb friction law with a friction coefficient of 0.1. The contact between the hammer and the specimen along with the anvils and the specimen was defined using the master–slave algorithm. The surfaces of hammer and anvils were defined as slave surface and the surface of the specimen was defined as a master surface. Loading was modelled by prescribing the initial velocity of the hammer. The anvils were defined to remain fixed whereas the impact hammer could only move vertically. The impact hammer had an initial velocity of 6.5m/s and a mass of 985kg. In general explicit codes are used to capture the complicated system response as a function of time. Currently, the ABAQUS Dynamic/Explicit solver does not support the use of XFEM. In this study this issue was overcome by using the Dynamic/Implicit solver.

Material parameters

An experimental true stress-strain curve of API X70 at -100°C was used to simulate the material behaviour of the DWTT specimen. It is worth to mention that in this study strain rate was not considered directly in the calculations of stress and strain fields. However, the strain rate does not have influence on the cohesive stress value in the case of brittle fracture.

The only part which is affected by strain rate is the cohesive energy (fracture energy). In this study the cohesive energy was calibrated using the data obtained by dynamic impact test as elaborated later on. Therefore, elastic-plastic material behaviour with isotropic hardening was defined. The enrichment area was chosen inside the area of interest for crack propagation which was the mesh refinement region.

Damage modelling allows simulation of crack initiation and eventual failure of the enriched area in the solution domain. The initial response is linear, while the failure mechanism consists of a damage initiation criterion and a damage propagation law. The damage initiation was defined based on the cohesive stress of Tmax=1.4σy. The cohesive stress was determined by studying the damage process at the micro-scale using the so-called unit cell method as suggested by Scheider [8]. At the notch tip, the stress triaxiality varies with the increase of impact loading. For the cohesive zone model, it results in a change of the cohesive stress which depends on the stress triaxiality. In this study, the maximum value of the stress triaxiality at the notch tip was used for evaluating the cohesive stress in the unit cell method. Using the unit cell method, the maximum load carrying capacity can be captured during the damage initiation process under the given stress triaxiality, and the value of the maximum load carrying capacity is equal to the cohesive stress. After obtaining the fracture toughness value using the CVN impact test, the characteristic strength was obtained by varying the maximum stress in the traction-separation law, while maintaining the toughness at a constant value [9]. This means that the damage initiation parameter was calibrated, until the best agreement was achieved between the experimental and numerical load displacement curves.

When the damage initiation criterion is met, the damage propagation law starts to take place. In this study, the damage evolution was defined in terms of fracture energy (per unit area). Therefore, the fracture energy (cohesive energy, Γ) was used for the damage evolution criteria. The cohesive energy was estimated using the relationship

$$\Gamma = G_{IC} = \frac{K_{IC}^2}{E/(1-\upsilon^2)} \tag{10}$$

where G_{IC} is the fracture energy, K_{IC} is the fracture toughness, E is the Young's modulus and υ is Poisson's ratio. The value for the fracture toughness was estimated from CVN energy. G_{IC} becomes the critical value of the rate of release in strain energy for the material which leads to damage evolution and possibly fracture of the specimen. The relationship between stress intensity and energy release rate is significant because it means that the G_{IC} condition is a necessary and sufficient criterion for crack propagation since it embodies both the stress and energy balance criteria. Barsom and Rolfe [10] suggested the correlation between CVN energy (KCV) and fracture toughness for the lower shelf of the DBTT curve, which is known as the Barsom-Rolfe correlation. They have examined the applicability of various regression models in order to monitor the empirical relationship of fracture toughness with other mechanical properties such as KCV. They have found that for KVC and yield stress in ranges of 4-82J and 270-1700MPa respectively, the following practical equation can be derived

$$K_{IC} = 6.76 \left(KCV \right)^{\frac{3}{4}} \tag{11}$$

In this study the mixed-mode behaviour was chosen and the fracture energies for those modes were introduced into XFEM. The fracture toughness values were selected as 25 MPa√m for Mode I and Mode II, respectively. The same values for cohesive stress and energy have been applied successfully to CVN simulation in the author's previous work [6].

RESULTS AND DISCUSSION

Model validation

In order to validate the developed model, results of the finite element simulation were compared with the experimental data. Fig. 3(a) and (b) depict the comparison of force against hammer displacement and absorbed energy between simulation and experiment. From the figure it can be seen that the simulation slightly overestimates the contact force. However, the estimated results were close enough to the experimental observation. By comparing the amount of observed energy, which is the integrated area beneath the force-displacement curve as shown in Fig. 3(b), between the calculated simulation results and the observed experimental data, it can be noticed that the numerical predicted data is in a good agreement with the measured data. Fig. 4 depicts that as the crack propagates, the maximum

stress distribution extends along the loading direction till the middle of the specimen and mode I fracture occurs. Then the mixed mode behaviour governs the failure mode.
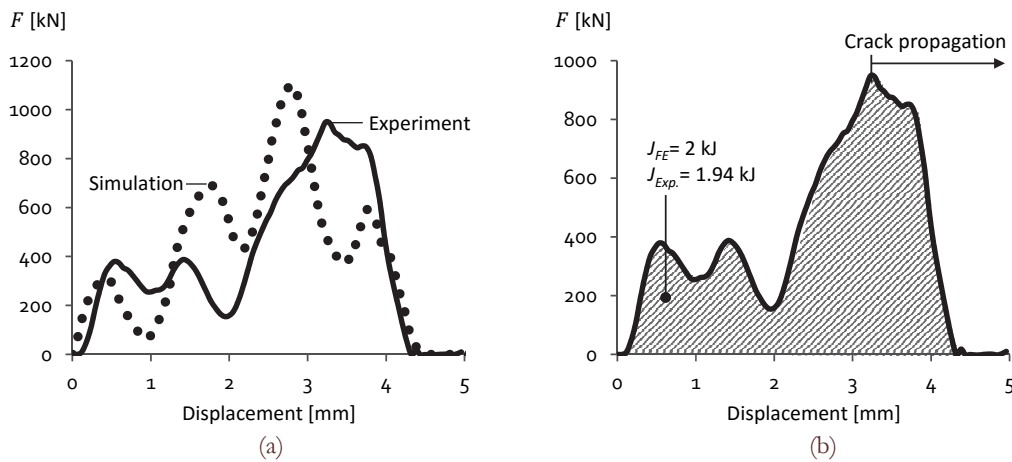

Figure 3: Comparison of force against hammer displacement and absorbed energy between simulation result and experimental observation.
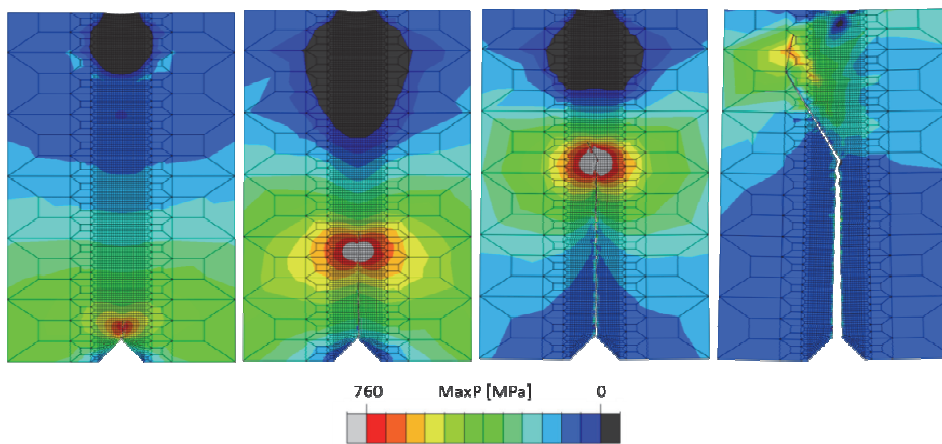

Figure 4: Maximum principle stress (MaxP) distribution during crack propagation steps.

From the simulation result, it was noticed that, the XFEM-based cohesive segment approach can be a suitable methodology to model brittle fracture behaviour of API X70 pipeline steels. Nevertheless, due to the strong discontinuous behaviour of the XFEM crack propagation process, the possibilities of facing numerical convergence issues are very high. Up to ABAQUS 6.13 version this convergence issue is related to the XFEM implementation inside ABAQUS, which is not responding perfectly under dynamic loading conditions. Moreover, an enriched element cannot be intersected by more than one crack.

Dynamic stress intensity factor calculation

The dynamic stress intensity factor (K_{ID}) can be determined using different experimental approaches. Nishioka and Atluri [11] have introduced an optimum technique for determining the dynamic stress intensity factor through the measurement of the Crack Mouth Opening Distance (δ_{CMOD}), applying the well-known relationship as in static conditions. Following the same approach as proposed by Nishioka and Atluri [11], the dynamic stress intensity factor was calculated from the FE results as:

$$K_{ID} = \frac{E\delta_{CMOD}}{\beta\sqrt{a\alpha}} \frac{C_1(\alpha)}{C_2(\alpha)} \qquad (12)$$

where a is the crack length, β is the span-to-width ratio ($\beta = S/W$, shown in Fig. 2), α is the crack-to-width ratio ($\alpha = a/W$, and $C_1(\alpha)$ and $C_2(\alpha)$ are non-dimensional functions depending on α and β values that can be found in Guinea et al. [12]. For the geometry considered in the present work these functions can be written as:

$$C_1(\alpha) = \frac{\sqrt{\alpha}}{(1-\alpha)^{1.5}(1+3\alpha)}\left(1.9 + 0.41\alpha + 0.51\alpha^2 - 0.17\alpha^3\right) \tag{13}$$

$$C_2(\alpha) = 0.76 - 2.28\alpha + 3.87\alpha^2 - 2.04\alpha^3 + \frac{0.66}{(1-\alpha)^2} \tag{14}$$

Fig. 5(a) illustrates the propagated crack through single mesh and the measured δ_{CMOD} of the DWTT model. Fig. 5(b) shows the variation of calculated dynamic stress intensity factor versus δ_{CMOD}. As it can be noticed the relationship between the stress intensity in dynamic mode is linear with the δ_{CMOD}.
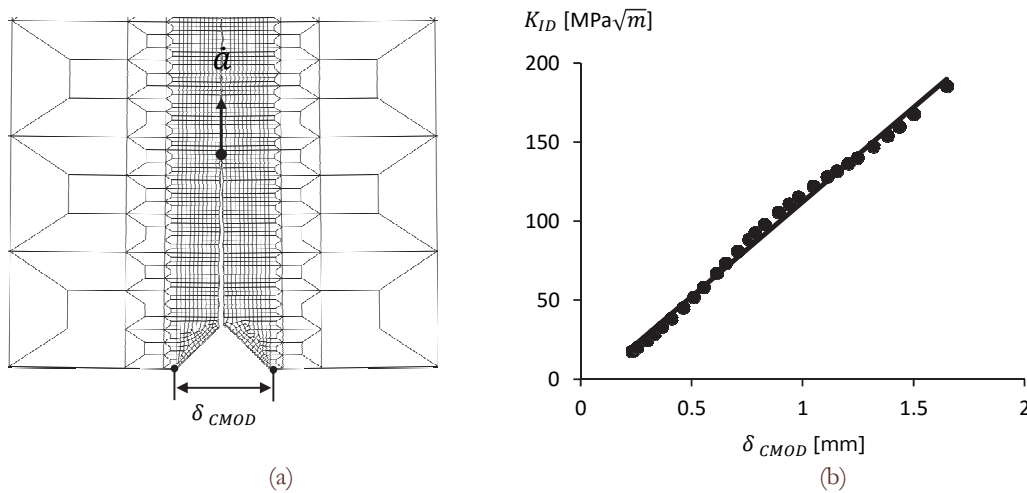

(a)   (b)

Figure 5: (a) propagating crack through single mesh of DWTT model and (b) calculated dynamic stress intensity factor versus Crack Mouth Opening Distance (δ_{CMOD}).

$$\dot{a} = c_1 \ln\left(\frac{K_{ID}}{\sigma_y\sqrt{a}}\right) + c_2$$
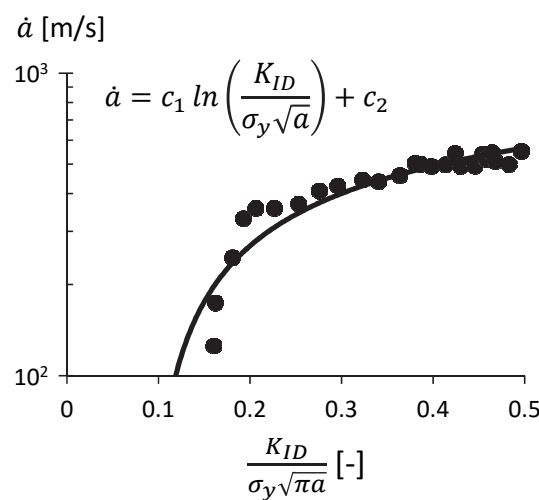
Figure 6: Calculated crack velocity versus normalized crack tip dynamic stress intensity factor.

Fig. 6 presents the variation of the measured crack propagation speed versus the normalized dynamic stress intensity factor calculated using Eq. 12. As it is shown in the figure the relationship between the crack propagation speed and the

normalized dynamic stress intensity factor is logarithmic for API X70 pipeline steel used in this investigation. These interesting results can be used for calculating the crack propagation speed in applications of CO_2 pipeline.

CONCLUSION

In this investigation dynamic fracture properties of CO2 pipeline steel were studied using the DWTT. The DWTT was simulated using the finite element modelling approach. To this end, the XFEM-based cohesive segment approach was implemented to model brittle fracture at low temperature, -100°C. After validation of the developed model against experimental observations significant results from the simulation were graphically presented and discussed. It was observed that the simulation overestimates the contact force. However, the simulation results and the experimental data were close enough to be reliable. To conclude, it was found that the XFEM-based cohesive zone approach is a suitable methodology to model brittle fracture behaviour of API X70 pipeline steels. However, due to strong discontinuous behaviour of the XFEM crack propagation process the possibility of facing numerical convergence issues are high. For future works the same approach can be implemented to study ductile or ductile-brittle behaviour of materials subjected to DWTT loading conditions in upper shelf or transition area, respectively.

ACKNOWLEDGMENTS

REFERENCES

[1] Andrews, R., Haswell, J., Cooper, R., Will fractures propagate in a leaking CO_2 pipeline?, J. Pipeline Eng., 9 (2010).

[2] Wu, Y., YU, H., Lu, C., Tieu, AK., Godbole, A., Michal, G., Transition of ductile and brittle fracture during DWTT by FEM, In: Proceedings of 13th international Conference on Fracture (ICF), (2013) 1648-1655.

[3] Scheider, I., Nonn, A., Völling, A., Mondry, A., Kalwa, C., A damage mechanics based evaluation of dynamic fracture resistance in gas pipelines, Procedia Mater. Sci., 31 (2014) 1956-64.

[4] Nonn, A., Wessel, W., Schmidt, T., Application of finite element analyses for assessment of fracture behavior of modern high toughness seamless pipeline steels, In: Proceedings of 23th International Offshore and Polar Engineering Conference, (2013).

[5] Catherine, C.S., Hourdequin, N., Galon, P., Forget, P., Finite element simulations of Charpy-V and sub-size Charpy tests for a low alloy RPV ferritic steel, In: Proceedings of 13th European Conference on Fracture (ECF13), (2000).

[6] Hojjati-Talemi, R., Cooreman S., Van Hoecke, D., Finite element simulation of dynamic brittle fracture in pipeline steel: A XFEM-based cohesive zone approach, Proc. Inst. Mech. Eng., Part L. DOI: 10.1177/1464420715627379.

[7] Belytschko, T., Black, T., Elastic crack growth in finite elements with minimal remeshing, Int. J. Numer. Methods. Eng., 45 (1999) 601-620.

[8] Scheider, I., Derivation of separation laws for cohesive models in the course of ductile fracture, Eng. Fract. Mech., 76 (2009) 1450-1759.

[9] Li, S., Thouless, M.D., Waas, A.M., Schroeder, J.A., Zavattieri, P.D., Use of a cohesive-zone model to analyze the fracture of a fiber-reinforced polymer-matrix composite, Compos. Sci. Technol., 65 (2005) 537-549.

[10] Barsom, J.M., Rolfe, S.T., Correlations between KIc and Charpy V-notch test results in the transition-temperature range. In: Impact Testing of metals, ASTM international, (1970). DOI: 10.1520/STP32067S.

[11] Nishioka, T., Atluri, S., A method for determining dynamic stress intensity factors from COD measurement at the notch mouth in dynamic tear testing, Eng. Fract. Mech., 16 (1982) 333-339.

[12] Guinea, G., Pastor, J., Planas, J., Elices, M., Stress intensity factor compliance and CMOD for a general three-point bend beam, Int. J. Fract., 89 (1998) 103–116.